

Phoenixin Attenuates Monosodium Glutamate-Induced Testicular Toxicity in Rats: A Potential Protective Approach

Mayada Mohamed Azab¹, Islam Ibrahim Hegab^{1,2}, Heba M. Shoeib³, Asmaa S. Mohamed³, Nancy Nagy Abed El-Hady⁴, Nesren Mohamed Mohamed¹.

1. Physiology Department, Faculty of Medicine, Tanta University, Tanta, Egypt.

2. Bio-Physiology Department, Ibn Sina National College for Medical Studies, Jeddah, Saudi Arabia.

3. Medical Biochemistry & Molecular Biology Department, Faculty of Medicine, Tanta University.

4. Anatomy and Embryology Department, Faculty of Medicine, Tanta University.

Submit Date : 11 April 2025

Revised Date : 03 May 2025

Accept Date : 12 June 2025

Keywords

- Phoenixin
- Monosodium Glutamate
- Testicular Toxicity

Abstract

Background: Monosodium glutamate (MSG), a widely utilized food additive, has been implicated in the provocation of testicular toxicity through oxidative stress and hormonal dysregulation. **Aim:** This study explores the potential role of phoenixin in ameliorating MSG-induced testicular toxicity. **Methods:** Forty male Wistar rats were randomly assigned to four distinct groups (n=10 per group): Control, Phoenixin, MSG, and Phoenixin+MSG, and were subjected to the experimental protocol over 30 days. Semen samples were analyzed for sperm count, motility, and viability. In serum, Gonadotropin-releasing hormone (GnRH), Luteinizing hormone (LH), follicle-stimulating hormone (FSH), testosterone, and kisspeptin were quantitatively assessed. The activity of the testicular steroidogenic enzymes 3 β -hydroxysteroid dehydrogenase (3 β -HSD) and 17 β -HSD, together with markers of testicular oxidative stress and tumor necrosis factor- α (TNF- α), were assessed. Additionally, the testicular levels of silent information regulator of transcription 1 (SIRT1), phosphorylated AMP-activated protein kinase (p-AMPK), and caspase-3 immunoreactivity were estimated. **Results:** MSG exposure significantly impaired sperm parameters, disrupted hormonal balance, and triggered oxidative stress and inflammatory responses in the MSG group compared to the Phoenixin and control groups. In contrast, co-administration of phoenixin in the Phoenixin+MSG group significantly restored sperm function, improved serum sex hormone profile, enhanced testicular antioxidant defenses, upregulated p-AMPK and SIRT1 expression, while attenuating TNF- α expression and caspase-3 immunoreactivity compared to the MSG group. Our findings underscore the pivotal role of phoenixin in ameliorating testicular dysfunction and promoting steroidogenic activity in our experimental model. **Conclusion:** Phoenixin effectively protected against MSG-provoked testicular toxicity through the restoration of the hypothalamic-pituitary-gonadal (HPG) axis, enhancement of steroidogenesis, attenuation of oxidative stress, inflammation, and apoptotic cascade, which was enforced by its upregulation of the SIRT1/AMPK signaling. These results imply a beneficial role of phoenixin in mitigating the reproductive dysfunction associated with MSG testicular toxicity.

Introduction

The reproductive systems of both males and females are highly vulnerable to a variety of harmful environmental factors. Poor nutrition, medical disorders, industrial pollutants, and food additives are among numerous factors that have been linked to the onset and progression of reproductive dysfunction [1].

The synthetic sodium salt monosodium glutamate (MSG) is made of glutamate, a non-essential amino acid. MSG is usually added to food to enhance its flavor and is typically utilized unlabeled in various culinary items. As a result, it is impossible to determine how much MSG a typical individual consumes daily [2]. Several biological systems are susceptible to elevated MSG levels; meanwhile, one extremely susceptible MSG target is the reproductive system. It is more vulnerable to peroxidative and excitotoxic damage because it contains large amounts of polyunsaturated fatty acids, glutamate receptor abundance, and low antioxidant reserves [3]. When given orally to rats, MSG results in oxidative glutamate damage, hemorrhage in the testes, and low sperm count [4].

Phoenixin, a recently discovered neuropeptide localized primarily in the hypothalamus, has an emerging role in regulating reproductive function, neuroprotection, energy homeostasis, and the gut-brain axis [5]. Phoenixin-14, a 14-amino acid version, is the most researched form of the new peptide hormone. The hypothalamus, along with other regions of the brain and peripheral tissues involving the reproductive system, possesses significant levels of its expression [5].

The axis between the hypothalamus, pituitary, and gonadal, which governs reproductive function, is regulated by phoenixin. The hypothalamus and pituitary gland express their receptor, GPR173 [6]. In addition, phoenixin was reported to act locally on the ovarian mitochondrial machinery and overexpress the gonadotropin-releasing hormone (GnRH) receptors, through which it could elevate the ability of ovarian cells to withstand oxidative, inflammatory, and apoptotic damage, with a sequel of alleviating obesity-induced reproductive impairment [7].

Although the literature on phoenixin's impact on testicular dysfunction is scarce, Yilmaz et al., [8] reported that phoenixin therapy could mitigate torsion-detorsion of the testes. The authors attributed the protective effect of phoenixin to its anti-inflammatory effect and antioxidative ability, highlighting the potential for further investigation into its therapeutic role in improving other forms of testicular injury.

The NAD-dependent deacetylase protein, SIRT1, controls several sperm biological functions, such as repair of DNA, survival of the cell, autophagy, apoptosis, and energy homeostasis through adenosine monophosphate-activated protein kinase (AMPK) activation [9]. As far as we are aware, there are no findings on how MSG and phoenixin affect the testicular SIRT1 and its signaling cascades.

These aforementioned data could provide a scientific rationale for considering phoenixin as a potential protective agent against MSG-induced testicular deterioration. The scarcity of scientific research examining phoenixin's preventive benefits

against testicular dysfunction linked to MSG further underscores the significance of our study in addressing this gap.

2. Materials and methods

2.1. Drugs and chemicals

Phoenixin-14 amide was procured from Sigma-Aldrich Corporation, headquartered in St. Louis, Missouri, USA. The MSG, a crystalline powder, was formulated by dissolving a measured amount in distilled water to achieve the designated concentration. All additional chemicals were sourced from Sigma Chemical Company (MO, USA).

2.2 Animals

In February 2025, a study was conducted at Tanta University using 40 albino rats (Wistar strain, males) with a weight range of 180 to 220 grams. The animals were distributed randomly into adequately ventilated cages, with five rats per enclosure, and housed under standardized conditions ($22 \pm 2^{\circ}\text{C}$ temperature and a 12-hour alternating light and dark schedule). For the entire duration of the study, the animals were provided unrestricted ad libitum access to a standard laboratory rodent diet and drinking water. The study protocols received ethical approval from the Medical Research Ethics Committee of Tanta University's Faculty of Medicine (Approval Code: [36264PR1050/1/25]).

2.3. Experimental design

Following a seven-day acclimation phase, the rats were randomly allocated into four experimental groups, each comprising ten animals, and subjected to daily treatments for 30 days in all groups:

- ***Group I (Control):** Received distilled water and isotonic saline daily via oral gavage.
- ***Group II (Phoenixin):** Received phoenixin at a dosage of 100 ng/g body weight after dissolution in sterile isotonic saline via gastric gavage daily, as established by [10].
- ***Group III (MSG):** Treated with monosodium glutamate (MSG) at a dosage of 3 g/kg/day after dissolution in distilled water via oral gavage, a regimen previously shown to induce testicular toxicity and reproductive impairment in rats as reported by [11, 12].
- ***Group IV (Phoenixin + MSG):** Received combined phoenixin and MSG treatments, following the same protocols as groups II and III, administered concurrently.

2.4. Experimental procedures

Upon completion of the 30-day experiment, rats were given an intraperitoneal (IP) injection of sodium pentobarbital administered at a dosage of 60 mg/kg [13], then were sacrificed via cervical dislocation. Blood was collected via cardiac puncture, then serum was collected and cryopreserved at -80°C for later biochemical testing.

Following this, a laparotomy was performed to excise the testes and epididymis. The organs were rinsed in 1.15% potassium chloride (KCl) solution at 0°C , dried completely, and weighed. The epididymal tissue was processed for *semen evaluation*. Seminal fluid specimens were obtained from the cauda region of the epididymis to evaluate sperm motility, concentration, and viability. The cauda region was surgically excised, weighed, and finely minced in 2 mL of physiological saline. The tissue was then

maintained at ambient temperature to allow spermatozoa to disperse into the saline solution [14].

Then, each testis was cut into three parts. The first part was homogenized in 1.15% KCl and centrifuged at (3000 rpm, 10 minutes, 4°C) to prepare supernatants for *biochemical analysis*. The second portion was maintained in a frozen state at -80°C for future *RNA extraction and molecular assay*. The third portion was preserved in Bouin's solution for 24 hours. Subsequently, the tissue was dehydrated using progressively concentrated ethanol solutions, cleared, and then embedded in paraffin. Thin sections (5 µm in thickness) were then sliced and stained with hematoxylin and eosin (H&E) for *histopathological* and *immunohistochemical assay*. Testicular protein levels were quantified using the Bradford method [15].

2.4.1 Sperm function evaluation:

-Formotility assessment, a droplet of the sperm sample was placed onto a microscope slide preheated to a temperature of 37 degrees Celsius. The proportion of motile sperm was analyzed via examining ten randomly selected fields at 400x magnification, with the average motility calculated using the methodology outlined in **Cheng et al.**[16]

-Sperm Viability Assessment: Seminal smears were prepared with eosin-nigrosin staining, a method described by **Filler** [17]. Microscopic analysis was performed to differentiate live (unstained) from dead (stained) spermatozoa, enabling the calculation of the viability percentage based on the alive-to-dead ratio.

-Sperm count analysis: The quantification of sperm count per milliliter was conducted following the protocol outlined by **Robb et al.** [18]. Semen samples were diluted at a 1:5 ratio (volume/volume) using normal saline supplemented with 40% formalin to immobilize spermatozoa. The total sperm count was subsequently determined using a Neubauer hemocytometer.

2.4.2 Biochemical assays:

2.4.2.1 Assessment of hormonal profile:

Serum levels of **Gonadotropin-releasing hormone** (GnRH) and **luteinizing hormone** (LH) were quantified using Enzyme-Linked Immunosorbent (ELISA) kits from LifeSpanBioSciences, Inc. (Washington, USA; Catalog No: LS-F13002 and LS-F27508, respectively). **Testosterone** was analyzed utilizing a kit from Aviva Systems Biology (San Diego, USA; Catalog No: OKEH02537), **follicle-stimulating hormone** (FSH) was determined by using a kit from Cloud-Clone Corp. (Houston, USA; Catalog No: CEA830Ra), and **Kisspeptin** was analyzed using a kit supplied by CUSABIO Life Science (Maryland, USA; Code: CSB-E13434r).

2.4.2.2 Assessment of testicular oxidative stress biomarkers:

Malondialdehyde (MDA), a recognized biomarker of oxidative lipid damage, was measured in testicular tissue homogenates using a thiobarbituric acid-based spectrophotometric technique, as outlined in the protocol by **Mihara and Uchiyama** [19]. Concurrently, the enzymatic activity of **glutathione peroxidase (GPx)**, an antioxidant enzyme, was evaluated by

Biodiagnostic Co.'s colorimetric assay kit** (Giza, Egypt, Catalog No:GP 2524) to assess antioxidant capacity. Furthermore, oxidative DNA damage was evaluated by quantifying the levels of 8-hydroxy-2'-deoxyguanosine (8-OHdG) in the homogenate via an ELISA kit (Catalog No: E-EL-0028, Elabscience, USA), providing insight into DNA oxidation.

2.4.2.3 Assessment of 3 β -hydroxysteroid dehydrogenase (3 β -HSD) and 17 β -HSD enzymes activity:

The enzymatic activity of 3 β -HSD and 17 β -HSD, critical enzymes in androgen synthesis and steroidogenic machinery, was measured in testicular homogenates using methodologies adapted from Talalay et al [20] and Jarabak et al [21], respectively.

2.4.2.4 Assessment of testicular p-AMPK levels:

Testicular phosphorylated AMP-activated protein kinase (p-AMPK) concentrations were quantified via an ELISA kit (Catalog No. MBS1602983, MyBioSource, San Diego, USA).

Table 1. Primer sequences for qRT-PCR.

Gene	GenBank Accession No.	Forward	Reverse
SIRT-1	NM_001372090.1	5'-GTG GCA GTA ACA GTG ACA GTG-3'	5'-GTC AGC TCC AGA TCC TCC AG-3'
TNF-α	NM_036807.1	5'-CCCTGGTACTAACTC CCAGAAA-3'	5'-TGTATGAGAGGGACGGAA CC-3'
GADPH	NM_017008.4	5'-CATGCCGCTGGAGAAACCTGCCA-3'	5'-GGGCTCCCCAGGCCCTC CTGT-3'.

The thermal cycling settings were: An initial step of activation, subsequent denaturation, annealing, and extension. The study analyzed quantitative PCR data by first determining the cycle threshold (Ct) measurements for the genes of interest. These values were normalized against the Ct of the

2.4.2.5 Real-time quantitative PCR (qPCR) of testicular SIRT-1 and tumor necrosis factor- α (TNF- α)

Extraction of total RNA from frozen testicular tissue using Thermo Scientific GeneJET RNA Purification Kit (comparable to Catalog No: K0731, Waltham, MA, USA) was carried out, followed by estimation of RNA concentration and purity using a NanoDrop spectrophotometer (NanoDrop Technologies, Inc., Wilmington, NC, USA).

The cDNA synthesis from 5 μ g of total RNA was performed using RevertAid H Minus Reverse Transcriptase (Thermo Scientific, Waltham, MA, USA; Catalog No: EP0451). Subsequently, 2 μ L of the resulting cDNA was amplified via SYBR Green-based quantitative PCR (qPCR) utilizing Applied Biosystems' StepOne Plus Real-Time PCR platform. The primer sequences utilized in the reactions are presented in **Table 1**.

housekeeping gene GAPDH to account for variations in sample loading. Relative gene expression was then quantified as fold change using the $2^{-\Delta\Delta C_t}$ formula, following the Livak method [22].

2.4.3 Histological study:

Both seminiferous tubules and interstitial spaces were included in the samples. Following a 24-hour fixation period in Bouin's solution, a tissue fragment was dried by a series of graded ethanol, cleared, and embedded in paraffin wax[23]. Serial paraffin sections were cut at 5 μ m thickness, stained by Hematoxylin and Eosin (H&E), and subjected to histopathological examination[24].

2.4.3.1 Immunohistochemical analysis for caspase 3

Following dewaxing and rehydration, paraffin-embedded tissue sections were washed with phosphate-buffered saline (PBS) for immunohistochemistry. The slides were incubated in a water bath maintained at 95–98°C for 20 minutes after being submerged in 10 mM sodium citrate buffer (pH 6.0) to retrieve the antigen. The slides underwent treatment using 3% hydrogen peroxide for 10 minutes at ambient temperature to stop the endogenous peroxidase activity. Following this, the slides underwent three PBS washes, each lasting five minutes [25].

The sections were treated with a rabbit-derived polyclonal antibody targeting caspase-3, an apoptosis biomarker (26) for a whole night at 4°C in a humidified incubation chamber (Abcam, Cambridge, MA, USA) with antibodies diluted at a ratio of 1:1000. The study then used the Avidin-Biotin-Peroxidase method for the immunohistochemistry identification of caspase-3 [27]. Tissue sections were treated without the main antibodies for negative controls [25]. Caspase-3-positive cells showed distinct brown cytoplasmic staining, indicating immunoreactivity [28].

2.5. Statistical analysis:

The data are presented as mean \pm standard deviation (SD). One-way analysis of variance (ANOVA) was employed to compare differences across multiple groups, with Tukey's post hoc test utilized for pairwise comparisons. Statistical significance was established at $P < 0.05$. Data analysis was performed using IBM SPSS Statistics software (Version 23.0, NY, USA)."

3. Results

3.1. Impact of phoenixin and MSG on semen analysis (sperm count, motility & viability)

Relative to the control and phoenixin groups, the MSG group's sperm count, motility, and viability were significantly lower. However, as Figure 1 illustrates, co-administration of phoenixin and MSG significantly mitigated these parameters in comparison to the MSG-treated group.

3.2. Impact of phoenixin and MSG on the HPG axis

As displayed in Figure 2, the MSG-treated rats' serum levels of GnRH, FSH, LH, testosterone, and Kisspeptin levels exhibited a significant decline relative to those of phoenixin and the control groups. In the meantime, these hormones were significantly raised by the simultaneous administration of MSG and phoenixin as opposed to the MSG group. According to these findings, Phoenixin intervention could reverse the disruption in the HPG axis, which was reflected by improvement of the MSG-induced reproductive dysfunction.

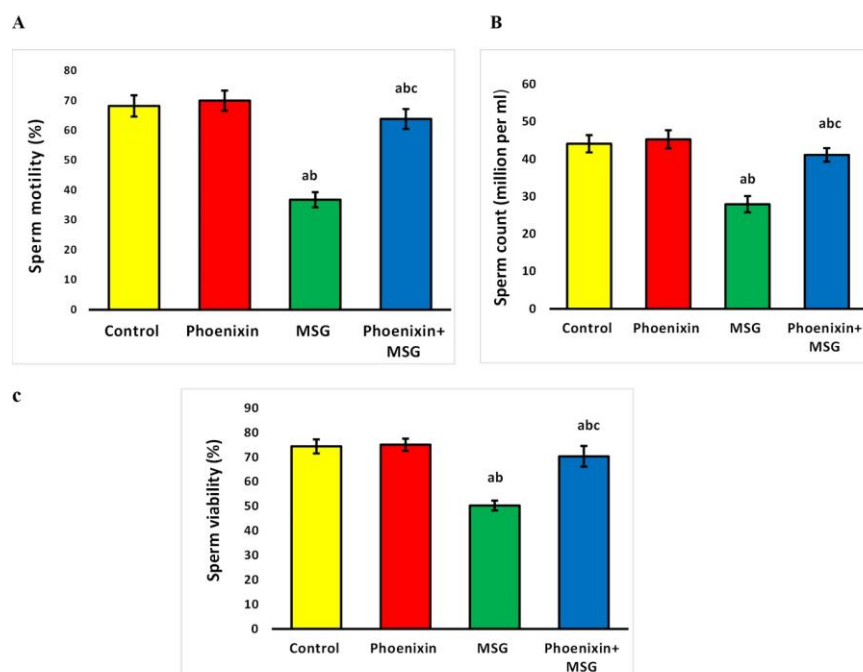


Figure 1. Impact of phenixin and MSG on semen analysis. (A) sperm motility, (B) sperm count, (C) sperm viability. Note: Data are presented as mean \pm SD (n = 10). ^a p<0.05 Vs. Control, ^bp<0.05 Vs Phenixin, ^c p<0.05 Vs. MSG group. MSG, monosodium glutamate.

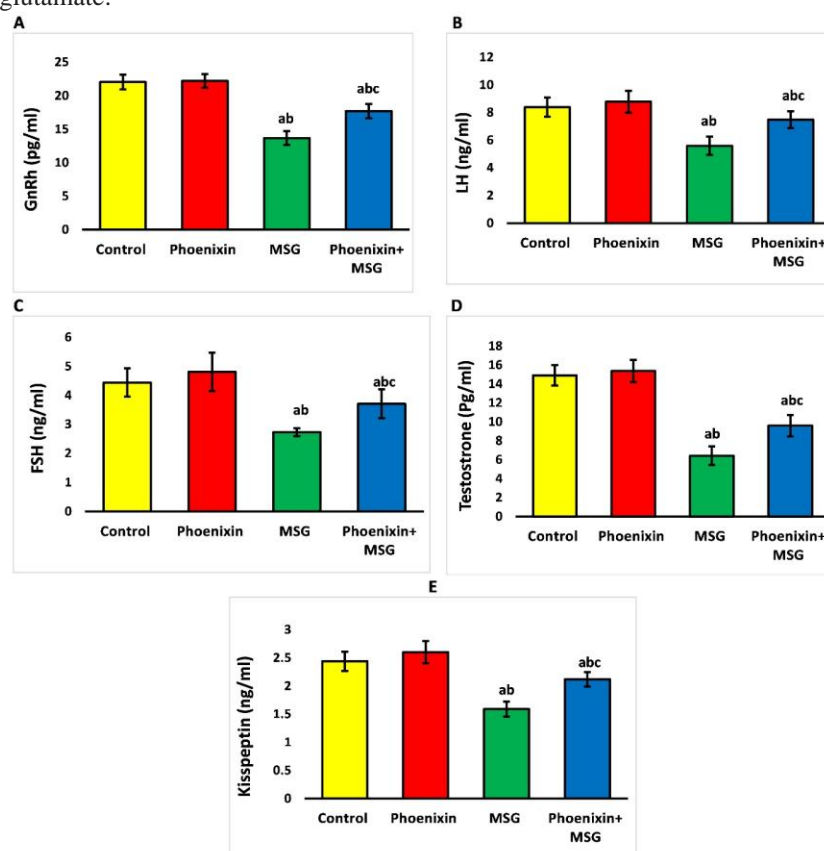


Figure 2. Influence of phenixin & MSG on HPG axis and kisspeptin levels. (A) GnRH, (B), LH (C), FSH (D) Testosterone, and (E) kisspeptin. Note: Data are expressed as mean \pm SD (n=10). ^a p <0.05 Vs. Control, ^bp<0.05 Vs Phenixin, ^c<0.05 Vs MSG group. MSG, monosodium glutamate; FSH, Follicle-Stimulating Hormone; LH, Luteinizing Hormone; GnRH, Gonadotropin-releasing hormone.

3.3. Impact of phoenixin and MSG on steroidogenic testicular enzymes (3B-HSD and 17B-HSD)

As displayed in Table 2 and comparable to the control and phoenixin groups, the MSG group's enzyme activities of 3B-HSD and 17B-HSD were significantly lower. However, rats given MSG and phoenixin together showed significantly greater 3B-HSD and 17B-HSD activity than those in the MSG group.

3.4. Phoenixin ameliorated MSG-induced testicular oxidative stress and inflammation

MSG supplementation for 30 days led to significantly greater levels of MDA, 8.OHdG, and TNF α , along with lower levels of GPx, in contrast to the phoenixin and control groups. But, as seen in Table 3, when phoenixin and MSG were given in combination, the previously mentioned characteristics were inverted.

3.5. Phoenixin reversed the MSG impact on the testicular SIRT1/AMPK axis

Comparable to the control and phoenixin groups, the MSG group demonstrated a significant downregulation of testicular SIRT1 and p-AMPK, as illustrated in Figure 3. In the meantime, this pathway was significantly upregulated when phoenixin and MSG were administered at the same time. This may lend credence to the idea that SIRT/AMPK plays a part in phoenixin's protection against MSG-induced testicular damage.

3.6 Impact of phoenixin on the testicular histological structure:

Histological analysis of testicular tissue from both the control and phoenixin groups demonstrated structurally normal seminiferous tubules in the testis (Figure 4 A-F). Seminiferous tubules were

rounded to oval and lined with stratified germinal epithelium. Their lumina are filled with mature spermatozoa. Interstitial tissue contains clusters of Leydig cells and seminiferous tubules with intact basement membranes. Sertoli cells and spermatogonia rest on the basement membrane. Seminiferous tubules are lined by spermatogonia, spermatocytes, and mature spermatids. Interstitial tissue contains clusters of Leydig cells, and seminiferous tubules are surrounded by myoid cells. There are large irregular pale nuclei of Sertoli cells, darkly stained spermatogonia, spermatocytes with large nuclei, round and elongated spermatids, and mature spermatozoa in the lumen.

However, the histological examination of the MSG group (Figure 4 G-I) demonstrated structural alterations in the seminiferous tubules, including irregular tubules, some appear with irregular germinal epithelium, and others show the separation of epithelium from the basement membrane. Eosinophilic material was noted within vacuolated Leydig cells. The lumen had few sperm with hypoplasia of the cells. The lumen had few sperm, and the interstitial tissue showed congested and dilated blood vessels. Spermatogenic cells showed cytoplasmic vacuolation and dark, small pyknotic nuclei. Wide intercellular spaces can be seen.

Meanwhile, the phoenixin + MSG group (Figure 4 J-L) exhibited restoration of the seminiferous tubule architecture, although intertubular spaces remained widened, and the spermatogenic cells appeared nearly normal. Stratified epithelium extends from the base to the lumen, with the lumen filled with slight edema between tubules.

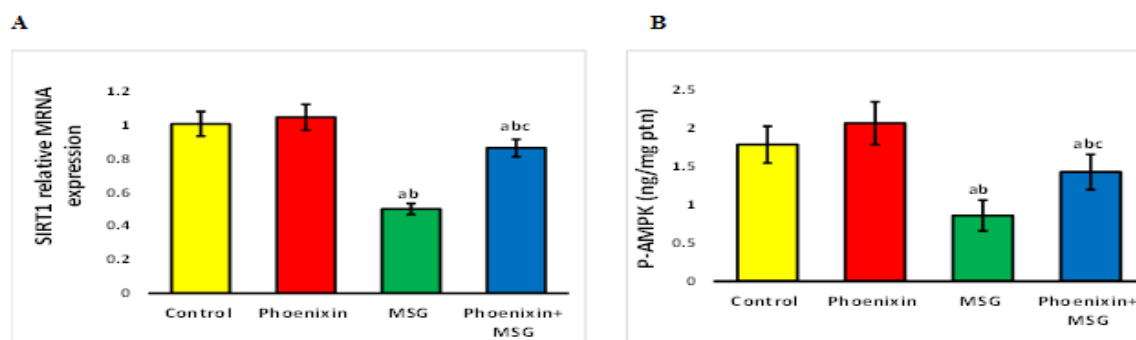


Figure 3. Impact of phenixin and MSG on the testicular SIRT/AMPK axis. (A) SIRT1 relative mRNA expression and (B) p-AMPK. Note: Data are stated as mean \pm SD (n = 10). ^a p<0.05 Vs. Control I, ^b p<0.05 Vs. Phenixin, ^c p<0.05 Vs. MSG group. MSG, monosodium glutamate, SIRT1: Silent information regulator 1, P-AMPK: phosphor-adenosine monophosphate-activated protein kinase.

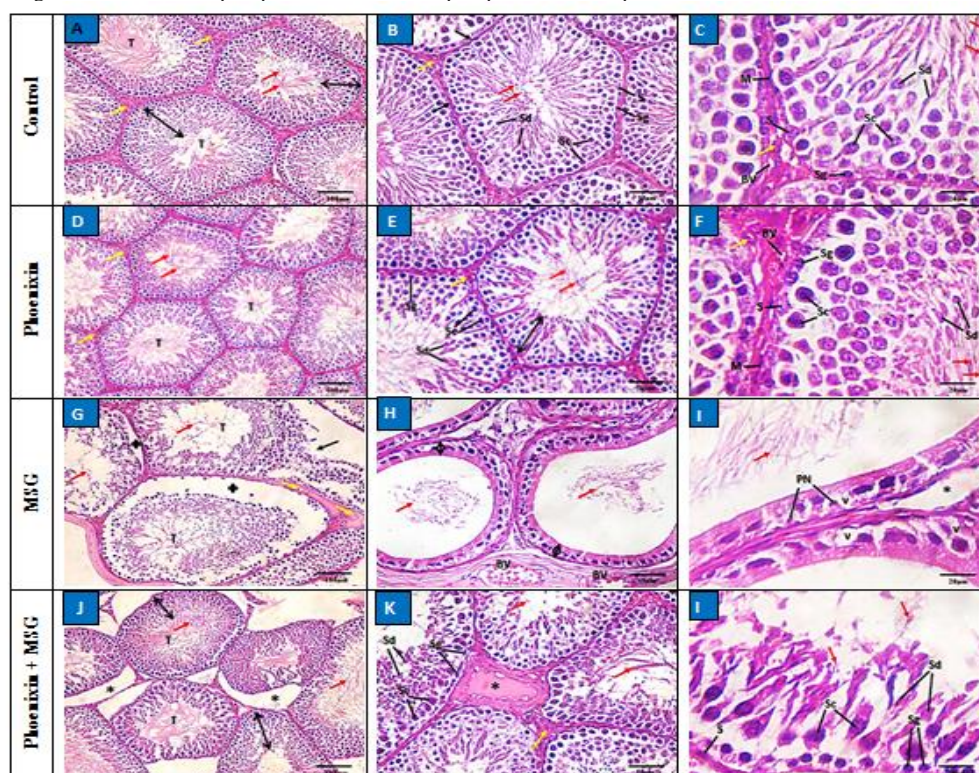


Figure 4: Histological examination of the testis from the groups studied. (A-C) **The control group** demonstrated: (A) Rounded to oval seminiferous tubules (T) lined with stratified germinal epithelium (double head black arrow). Their lumina are filled with mature spermatozoa (red arrows). Interstitial tissue containing clusters of Leydig cells (yellow arrows), (B) Seminiferous tubules with intact basement membrane (black arrows). Sertoli cells (S) and spermatogonia (Sg) rest on basement membrane. Seminiferous tubule lined by spermatogonia, spermatocytes (Sc), spermatids (Sd), and mature spermatozoa (red arrows). Interstitial tissue contains clusters of Leydig cells (yellow arrow), and (C) Seminiferous tubules are surrounded by myoid cells (M). There are large irregular pale nuclei of Sertoli cells (S), darkly stained spermatogonia (Sg), spermatocytes (Sc) with large nuclei, round and elongated spermatids (Sd), and mature spermatozoa (red arrows) in the lumen. Interstitial Leydig cells (yellow arrow) can be seen. (D-F) **Phenixin group** showed: (D) Seminiferous tubules (T) with lumen filled with spermatozoa (red arrows). Interstitial tissue contains clusters of Leydig cells (yellow arrows), (E) Spermatogenic cells extend from the base to the lumen (double-headed black arrow). There are spermatogonia (Sg), spermatocytes (Sc), spermatids (Sd), and spermatozoa in the lumen (red arrows). Interstitial tissue contains clusters of Leydig cells (yellow arrow), (F) Seminiferous tubule surrounded by myoid cells (M). There are irregular elongated pale nuclei of Sertoli cells (S) and darkly stained spermatogonia (Sg) resting on the basement membrane. Spermatocytes (Sc), round and elongated spermatids (Sd), and a lumen filled with spermatozoa (red arrows). The interstitial Leydig cells (yellow arrow) and blood vessels (BV) can be seen. (G-I) **The MSG group** showed: (G) Irregular tubules (T), one appears with irregular germinal epithelium (black arrow) and others show the separation of epithelium from the basement membrane (+). Eosinophilic material with vacuolated Leydig cells (yellow arrows). The lumen has few sperms (red arrows), (H) Hypoplasia of cells (double head black arrow). The lumen has few sperms (red arrows). Interstitial tissue has congested and dilated blood vessels (BV), (I) Spermatogenic cells show cytoplasmic vacuolation (V) and dark small Pyknotic nuclei (PN). Wide intercellular spaces (*) can be seen. The lumen has few or no sperms (red arrow). (J-L) **Phenixin + MSG group** showed: (J) Apparently normal tubules (T) with wide spaces (*). Stratified epithelium extends from base to lumen (double head black arrow). The lumen is filled with spermatozoa (red arrows), (K) Slight edema (*) between tubules. Spermatogonia (Sg), spermatocytes (Sc), spermatids (Sd), and a lumen filled with spermatozoa (red arrows). Interstitial tissue contains clusters of Leydig cells (yellow arrow), (L) Sertoli cells (S), basal darkly stained spermatogonia (Sg), large spermatocytes (Sc), rounded or oval spermatids (Sd) and mature spermatozoa (red arrows). Hematoxylin and eosin staining (A, D, G & J) ($\times 200$, scale bar = 100 μ m), (B, E, H & K) ($\times 400$, scale bar = 50 μ m) and (C, F, I & L) ($\times 1000$, scale bar = 20 μ m).

3.7 Impact of phoenixin on the testicular caspase-3 immunohistochemistry

Immunohistochemical analysis of specimens from the control and phoenixin groups revealed negative caspase-3 immunostaining in spermatogenic cells. Conversely, the MSG group exhibited strong positive caspase-3

immunostaining within all spermatogenic cell layers in most of the seminiferous tubules, meanwhile, the Phoenixin + MSG group showed variable reaction to immunostaining. Some spermatogenic cells have negative reactions, while others appear with positive reactions, as displayed in **Figure 5**.

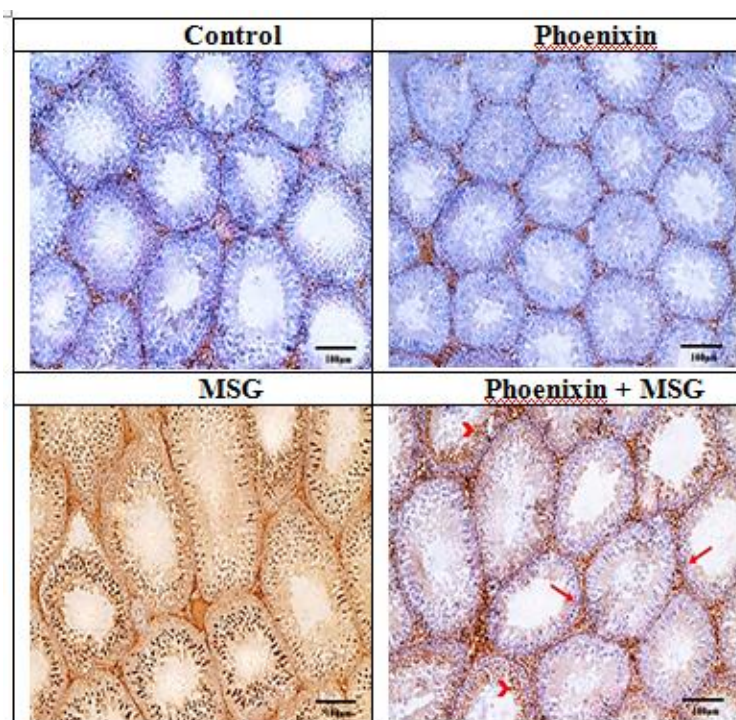


Figure 5: Photomicrograph of caspase-3 immunostaining in the rats' testes demonstrated the protective role of phoenixin against MSG-induced testicular injury. **Control and Phoenixin groups** exhibited negative caspase-3 immunostaining in spermatogenic cells, the **MSG group** showed strong positive caspase-3 immunostaining within all spermatogenic cell layers in most of the seminiferous tubules, meanwhile, the **Phoenixin + MSG** group showed variable reaction to immunostaining. Some spermatogenic cells show negative reactions (arrows), while others appear with positive reactions (arrow heads). Original magnification x100, scale bar 200 µm.

4. Discussion:

The foremost outcome of our research is that the HPG axis imbalance, coupled with inflammatory, oxidative stress, and apoptotic cascade, could be the main fundamental causes of MSG-induced testicular toxicity. Meanwhile, the simultaneous administration of phoenixin and MSG could alleviate the MSG-provoked testicular toxicity, as evidenced by the mitigation of the disturbed hormonal profile, testicular architecture, and sperm analysis parameters.

Our results showed that MSG signified a real challenge for spermatogenesis, as revealed by the MSG group's deteriorated sperm parameters relative to the control group.

Impaired spermatogenesis may result from inherent issues within germ cells, supporting Sertoli cells, or Leydig cells, or it may be attributed to the disrupted endocrine signals that regulate the entire spermatogenetic process [29].

At the central level, our findings highlighted that MSG interferes with the normal functioning of the HPG axis, mirrored by reduced serum GnRH, FSH, LH, and testosterone, which are mandatory for normal spermatogenesis and testicular function. This is most likely a consequence of excitotoxic neuronal destruction in the hypothalamus that could be a sequel of excess stimulation of N-methyl-D-aspartic acid (NMDA) receptors [30]. This diminishes hypothalamic GnRH secretion, leading to a lack of LH and FSH, which negatively impacts testosterone production and spermatogenesis. MSG could act peripherally due to the existence of glutamate transporters and receptors within the testicular tissue. The expression of glutamateNMDA receptor, GluR1, GluR2/3, GluR2/3, and GluR5 mRNA has been documented in testicular tissue [31]

On the other hand, cotreatment with MSG and phoenixin successfully restored the functional integrity of the HPG axis, with a notable increase in GnRH secretion, which enhanced the gonadotropin production, as earlier supported [32]. Phoenixin enhanced GnRH's capacity to upregulate GnRH receptor expression in cultured dispersed male anterior pituitary cells, thus enhancing gonadotropin secretion [33].

In addition, the stimulatory effect of phoenixin on the GnRH release could be mediated by its enhancement in kisspeptin release, as evinced herein and previously supported [34]. Kisspeptin is a hypothalamic neuropeptide that responds to paracrine cues from dynorphin and neurokinin B, acting upstream of GnRH to stimulate its release. It also increases LH production and LH pulsatile frequency [35]. Phoenixin acts through the

GPR173 receptor to activate both GnRH and kisspeptin neurons, leading to increased expression of Kiss1, which can restore the release of GnRH and enhance FSH and LH secretion [36].

At the testicular level, our study found that the MSG group displayed a substantially declined testicular activity of 3 β -HSD and 17 β -HSD enzymes, which are crucial in testosterone synthesis. The reduced activity of these enzymes contributed to the decline in serum testosterone levels, confirming our hormonal findings. In contrast, phoenixin substantially stimulated their enzyme activities, which could play a role in improving testosterone secretion.

This could be mediated via its SIRT1 upregulation by phoenixin, as demonstrated by our findings presented later herein. Sirt1 modulates autophagy to control testosterone production in Leydig cells [37]. Sirt1 also promotes steroidogenesis via its anti-inflammatory effects and its coactivation of steroidogenic factor 1 [38]. Nevertheless, the specific molecular mechanism through which phoenixin influences the testosterone synthesis pathway remains unclear and warrants further investigation.

The testicular oxidative stress provoked by glutamate was validated herein by the notable increase in MDA and 8-OHdG levels concomitant with a decline in testicular GPx activity, as matched previously [39]. The MSG-induced ROS production is incremental in the testicular cellular damage and mitochondrial dysfunction [40]. The toxic effects of MSG can alter mitochondrial inner membranes, causing depletion of GSH levels, altering the oxidative defense systems, and

increasing lipid peroxidation. Testicular and sperm membranes are extremely vulnerable to reactive oxygen species, contributing to male infertility [41].

The MSG's pro-apoptotic activity was evinced herein by an increment of caspase 3 immun-expression at staggering levels within the testicular tissues of MSG-exposed rats. This is linked to excessive glutamate intake, which over-activates glutamate receptors, leading to intracellular calcium waves and triggering apoptosis [42]. MSG-induced oxidative stress also provokes apoptotic cell death with a sequel of testicular tissue damage [43]. The heightened apoptotic cell death in Leydig cells results in a reduction in testosterone production, potentially exacerbating germ cell apoptosis and increasing the risk of infertility [44].

In addition, our findings revealed significantly elevated levels of TNF- α in MSG-administered rats, which might be crucial in testicular dysfunction brought on by MSG. In harmony, **Leiseganget al.** [45] suggested a positive correlation between elevated levels of inflammatory cytokines and adverse effects on male reproductive function, such as disruption of the HPG axis and impairment of the steroidogenesis cascade, leading to hypogonadotropic hypogonadism."

On the other hand, and in alignment with previous studies [7, 8, 46], our findings demonstrate that phoenixin intervention signified a substantial antioxidant, antiapoptotic, and anti-inflammatory criterion, which could explain its testicular cytoprotection in the MSG-intoxicated rats. In

harmony, **Yilmaz et al.**'s recent study [8] revealed that the potent antioxidant and anti-inflammatory potentials of phoenixin alleviated the testicular damage provoked by torsion-detorsion in rats, raising the assumption of the potential therapeutic role of phoenixin in other models of testicular tissue damage.

Importantly, and considering our findings, we could hypothesize that the testicular protective impact of phoenixin could be mediated by its ability to counteract the MSG-induced downregulation of the SIRT1/AMPK signaling. This signifies the possible crucial role of this pathway in mediating the protective role of phoenixin in our model.

SIRT1 is fundamental for normal spermatogenesis and the protection of germ cells against the hazardous impacts of oxidative stress and apoptosis [47,48]. Its activation leads to the deacetylation of key transcription factors, thus enhancing cellular resilience against oxidative and inflammatory insults [5]. It activates and phosphorylates AMPK, which controls many cellular metabolic processes [49]. Both molecules activate each other to enhance mitochondrial biogenesis and display antioxidant criteria [49]. p-AMPK enhances ATP production, impacting sperm motility and acrosomal reaction while decreasing reactive oxygen species [50].

In harmony, **Zeng et al.** [51] documented that the modifying role of phoenixin on neuroinflammation and apoptotic cell death is SIRT1 dependent. Phoenixin demonstrated multiple hepatoprotective benefits, including anti-inflammatory and antioxidant potential, by activating the

AMPK/SIRT1 and NRF2/HO-1 pathways [10], aligning with our findings.

5. Conclusion

This research illustrated for the first time the phoenixin's role in mitigating both morphological and functional testicular derangements associated with MSG consumption. These protective effects were mediated through the ability to restore the HPG hormonal balance and steroidogenic machinery while promoting redox homeostasis, exerting anti-inflammatory and anti-apoptotic effects, and upregulating the SIRT1/AMPK signaling. These findings demonstrated phoenixin's imprint signature in combating the MSG-induced testicular damage and its associated reproductive aberrations and provide compelling evidence for further investigation into its additional mechanisms in testicular protection.

6. Declarations and statements Ethics approval and consent to participate:

We conducted the study protocol according to The Local Committee of Research and Medical Ethics of the Faculty of Medicine, Tanta University.

Availability of data and material:

The corresponding author can provide the datasets used and/or analyzed during the current work upon request.

Competing interests:

The authors declare to have no conflicts of interest.

Funding:

The authors received no specific funding for this work.

References:

1. Barbagallo F, La Vignera S, Cannarella R, Mongioì LM, Garofalo V, Leanza C, Marino M, Calogero AE, Condorelli RA. Obesity and male reproduction: do sirtuins play a role?. *International journal of molecular sciences*. 2022 Jan 16;23(2):973.
2. Hamza RZ, Al-Salmi FA, Laban H, El-Shenawy NS. Ameliorative role of green tea and zinc oxide nanoparticles complex against monosodium glutamate-induced testicular toxicity in male rats. *Current Pharmaceutical Biotechnology*. 2020 May 1;21(6):488-501.
3. Jubaidi FF, Mathialagan RD, Noor MM, Taib IS, Budin SB. Monosodium glutamate daily oral supplementation: Study of its effects on male reproductive system on rat model. *Systems biology in reproductive medicine*. 2019 May 4;65(3):194-204.
4. Khaled FA, Yousef MI, Kamel KI. The protective role of propolis against the reproductive toxicity of mono-sodium glutamine in male rabbits. *IJCS*. 2016;4(2):4-9.
5. Liang H, Zhao Q, Lv S, Ji X. Regulation and physiological functions of phoenixin. *Frontiers in Molecular Biosciences*. 2022 Aug 25;9:956500.
6. Pałasz A, Tyszkiewicz-Nwafor M, Suszka-Świtek A, Bacopoulou F, Dmitrzak-Węglarz M, Dutkiewicz A, Słopeń A, Janas-Kozik M, Wilczyński

- KM, Filipczyk Ł, Bogus K. Longitudinal study on novel neuropeptides phoenixin, spexin and kisspeptin in adolescent inpatients with anorexia nervosa—association with psychiatric symptoms. *Nutritional neuroscience*. 2021 Nov 2;24(11):896-906.
7. Basha EH, Eltokhy AK, Eltantawy AF, Heabah NA, Elshwaikh SL, El-Harty YM. Linking mitochondrial dynamics and fertility: Promoting fertility by phoenixin through modulation of ovarian expression of GnRH receptor and mitochondrial dynamics proteins DRP-1 and mfn-2. *Pflügers Archiv-European Journal of Physiology*. 2022 Oct;474(10):1107-19.
8. Yilmaz N, Hudaykulyeva J, Gul S. Phoenixin-14 may ameliorate testicular damage caused by torsion-detorsion by reducing oxidative stress and inflammation in prepubertal rats. *Tissue and Cell*. 2024 Jun 1;88:102405.
9. Liu H, Zhang S, Liu C, Wu J, Wang Y, Yuan L, Du X, Wang R, Marwa PW, Zhuang D, Cheng X. Resveratrol ameliorates microcystin-LR-induced testis germ cell apoptosis in rats via SIRT1 signaling pathway activation. *Toxins*. 2018 Jun 9;10(6):235.
10. Yang F, Huang P, Shi L, Liu F, Tang A, Xu S. Phoenixin 14 inhibits high-fat diet-induced non-alcoholic fatty liver disease in experimental mice. *Drug Design, Development and Therapy*. 2020 Sep 22:3865-74.
11. Anbarkeh FR, Baradaran R, Ghandy N, Jalali M, Nikraves MR, Soukhtanloo M. Effects of monosodium glutamate on apoptosis of germ cells in testicular tissue of adult rat: An experimental study. *International journal of reproductive biomedicine*. 2019 Apr;17(4):261.
12. Koohpeyma F, Gholizadeh F, Hafezi H, Hajiaghayi M, Siri M, Allahyari S, Maleki MH, Asmari N, Bayat E, Dastghaib S. The protective effect of L-carnitine on testosterone synthesis pathway, and spermatogenesis in monosodium glutamate-induced rats. *BMC Complementary Medicine and Therapies*. 2022 Oct 13;22(1):269.
13. Shekarforoush S, Fatahi Z, Safari F. The effects of pentobarbital, ketamine—pentobarbital and ketamine—xylazine anesthesia in a rat myocardial ischemic reperfusion injury model. *Laboratory animals*. 2016 Jun;50(3):179-84.
14. Saadeldin IM, Fadel AM, Hamada MM, El-Badry AA. Effects of exposure to 50 Hz, 1 Gauss magnetic field on reproductive traits in male albino rats. *Acta Veterinaria Brno*. 2011 Apr 12;80(1):107-11.
15. Bradford MM. A rapid and sensitive method for the quantitation of microgram quantities of protein utilizing the principle of protein-dye binding. *Analytical biochemistry*. 1976 May 7;72(1-2):248-54.
16. Cheng D, Zheng XM, Li SW, Yang ZW, Hu LQ. Effects of epidermal growth factor on sperm content and motility of rats with

- surgically induced varicoceles. *Asian Journal of Andrology*. 2006 Nov;8(6):713-7.
17. Filler R. Methods for evaluation of rat epididymal sperm morphology. *Methods in Toxicology*. 1993;3:334-43.
18. Robb GW, Amann RP, Killian GJ. Daily sperm production and epididymal sperm reserves of pubertal and adult rats. *Reproduction*. 1978 Sep 1;54(1):103-7.
19. Mihara M, Uchiyama M. Determination of malonaldehyde precursor in tissues by thiobarbituric acid test. *Analytical biochemistry*. 1978 May 1;86(1):271-8.
20. Talalay P. [69] Hydroxysteroid dehydrogenases: Hydroxysteroid+DPN+(TPN+)⇌ Ketosteroid DPNH (TPNH)+ H+. In *Methods in enzymology* 1962 Jan 1; 5:512-526. Academic Press.
21. Jarabak J, Adams JA, Williams-Ashman HG, Talalay P. Purification of a 17 β -hydroxysteroid dehydrogenase of human placenta and studies on its transhydrogenase function. *Journal of Biological Chemistry*. 1962 Feb 1;237(2):345-57.
22. Livak KJ, Schmittgen TD. Analysis of relative gene expression data using real-time quantitative PCR and the 2- $\Delta\Delta$ CT method. *methods*. 2001 Dec 1;25(4):402-8.
23. Yalçın T, Kaya S, Tektemur NK, Ozan İE. The methods used in histopathological evaluation of testis tissues. *Batman Üniversitesi Yaşam Bilimleri Dergisi*, 2020 10(1): 148-157.
24. Bancroft JD, Layton C. The hematoxylin and eosin. In: Suvarna SK, Layton C, Bancroft JD, editors. *Bancroft's theory and practice of histological techniques* 8th ed. Amsterdam, Netherlands: Elsevier. 2019: 126–138.
25. Goto S, Morigaki R, Okita S, Nagahiro S, Kaji R. Development of a highly sensitive immunohistochemical method to detect neurochemical molecules in formalin-fixed and paraffin-embedded tissues from autopsied human brains. *Frontiers in neuroanatomy*. 2015 Mar 3;9:22.
26. Barranco I, Gómez-Laguna J, Rodríguez-Gómez IM, Salguero FJ, Pallarés FJ, Bernabé A, Carrasco L. Immunohistochemical detection of extrinsic and intrinsic mediators of apoptosis in porcine paraffin-embedded tissues. *Veterinary Immunology and Immunopathology*. 2011 Feb 15;139(2-4):210-6.
27. Sayed AE, Abd-Elkareem M, Abou Khalil NS. Immunotoxic effects of 4-nonylphenol on *Clarias gariepinus*: Cytopathological changes in hepatic melanomacrophages. *Aquatic Toxicology*. 2019 Feb 1;207:83-90.
28. Zayed AE, Saleh A, Gomaa AM, Abd-Elkareem M, Anwar MM, Hassanein KM, Elsherbiny MM, Kotb AM. Protective effect of Ginkgo biloba and magnetized water on nephropathy in induced type 2 diabetes in rat. *Oxidative medicine and cellular longevity*. 2018;2018(1):1785614.

29. Kolthur-Seetharam U, Teerds K, de Rooij DG, Wendling O, McBurney M, Sassone-Corsi P, Davidson I. The histone deacetylase SIRT1 controls male fertility in mice through regulation of hypothalamic-pituitary gonadotropin signaling. *Biology of reproduction*. 2009 Feb 1;80(2):384-91.
30. Tripathi R, Samadder T, Gupta S, Surolia A, Shaha C. Anticancer activity of a combination of cisplatin and fisetin in embryonal carcinoma cells and xenograft tumors. *Molecular cancer therapeutics*. 2011 Feb 1;10(2):255-68.
31. Storto M, Sallese M, Salvatore L, Poulet R, Condorelli DF, Dell Albani P, Marcello MF, Romeo R, Piomboni P, Barone N, Nicoletti F. Expression of metabotropic glutamate receptors in the rat and human testis. *Journal of endocrinology*. 2001 Jul 1;170(1):71-8.
32. Guvenc G, Altinbas B, Kasikci E, Ozyurt E, Bas A, Udum D, Niaz N, Yalcin M. Contingent role of phoenixin and nesfatin-1 on secretions of the male reproductive hormones. *Andrologia*. 2019 Dec;51(11): e13410.
33. Yosten GL, Lyu RM, Hsueh AJ, Avsian-Kretchmer O, Chang JK, Tullock CW, Dun SL, Dun N, Samson WK. A novel reproductive peptide, phoenixin. *Journal of neuroendocrinology*. 2013 Feb;25(2):206-15.
34. Valsamakis G, Arapaki A, Balafoutas D, Charmandari E, Vlahos NF. Diet-induced hypothalamic inflammation, phoenixin, and subsequent precocious puberty. *Nutrients*. 2021 Sep 29;13(10):3460.
35. Prashar V, Arora T, Singh R, Sharma A, Parkash J. Hypothalamic Kisspeptin neurons: integral elements of the GnRH system. *Reproductive Sciences*. 2023 Mar;30(3):802-22.
36. Treen AK, Luo V, Belsham DD. Phoenixin activates immortalized GnRH and kisspeptin neurons through the novel receptor GPR173. *Molecular Endocrinology*. 2016 Aug 1;30(8):872-88.
37. Khawar MB, Liu C, Gao F, Gao H, Liu W, Han T, Wang L, Li G, Jiang H, Li W. Sirt1 regulates testosterone biosynthesis in Leydig cells via modulating autophagy. *Protein & cell*. 2021 Jan;12(1):67-75.
38. Wu L, Zhang A, Sun Y, Zhu X, Fan W, Lu X, Yang Q, Feng Y. Sirt1 exerts anti-inflammatory effects and promotes steroidogenesis in Leydig cells. *Fertility and sterility*. 2012 Jul 1;98(1):194-9.
39. Al-Shahari EA, El-Kott AF. Potential effect of grape seeds extract against monosodium glutamate induced infertility in rats. *Int J Pharmacol*. 2019;15(2):287–294.
40. Abdou HM, Hassan EH, Aly RG. Monosodium glutamate (MSG): promoter of neurotoxicity, testicular impairment, inflammation and apoptosis in male rats. *Swed J BioSci Res*. 2020;1(2):78-90.
41. Hamza RZ, Al-Harbi MS. Monosodium glutamate induced testicular toxicity and the possible ameliorative role of vitamin E

- or selenium in male rats. *Toxicology reports*. 2014 Jan 1;1:1037-45.
42. Abd-Elkareem M, Abd El-Rahman MA, Khalil NS, Amer AS. Antioxidant and cytoprotective effects of *Nigella sativa* L. seeds on the testis of monosodium glutamate challenged rats. *Scientific reports*. 2021 Jun 29;11(1):13519.
43. Kianifard D, Shoar SM, Karkan MF, Aly A. Effects of monosodium glutamate on testicular structural and functional alterations induced by quinine therapy in rat: An experimental study. *International Journal of Reproductive BioMedicine*. 2021 Feb;19(2):167.
44. Chen Z, Wen D, Wang F, Wang C, Yang L. Curcumin protects against palmitic acid-induced apoptosis via the inhibition of endoplasmic reticulum stress in testicular Leydig cells. *Reproductive Biology and Endocrinology*. 2019 Dec;17:1-0.
45. Leisegang K, Henkel R, Agarwal A. Obesity and metabolic syndrome associated with systemic inflammation and the impact on the male reproductive system. *American journal of reproductive immunology*. 2019 Nov;82(5):e13178.
46. Zandeh-Rahimi Y, Panahi N, Hesaraki S, Shirazi-Beheshtiha SH. Protective effects of phoenixin-14 peptide in the indomethacin-induced duodenal ulcer: An experimental study. *International Journal of Peptide Research and Therapeutics*. 2022 Jan;28(1):43.
47. Cora MC, Kooistra L, Travlos G. Vaginal cytology of the laboratory rat and mouse: review and criteria for the staging of the estrous cycle using stained vaginal smears. *Toxicologic pathology*. 2015 Aug;43(6):776-93.
48. Kianifard D, Shoar SM, Karkan MF, Aly A. Effects of monosodium glutamate on testicular structural and functional alterations induced by quinine therapy in rat: An experimental study. *International Journal of Reproductive BioMedicine*. 2021 Feb;19(2):167.
49. Price NL, Gomes AP, Ling AJ, Duarte FV, Martin-Montalvo A, North BJ, Agarwal B, Ye L, Ramadori G, Teodoro JS, Hubbard BP. SIRT1 is required for AMPK activation and the beneficial effects of resveratrol on mitochondrial function. *Cell metabolism*. 2012 May 2;15(5):675-90.
50. Nguyen TM. Impact of 5'-AMP-activated protein kinase on male gonad and spermatozoa functions. *Frontiers in Cell and Developmental Biology*. 2017 Mar 23;5:25.
51. Zeng X, Li Y, Ma S, Tang Y, Li H. Phoenixin-20 ameliorates lipopolysaccharide-induced activation of microglial NLRP3 inflammasome. *Neurotoxicity Research*. 2020 Oct;38:785-92.